Experimental characterization of electrodeless plasma thrusters for very low Earth Orbit applications

Andrés Rabuñal-Gayo

Supervisors: Jaume Navarro-Cavallé & Pablo Fajardo Peña

PhD Doctoral Meetings 2025. PhD program in Aerospace Engineering UC3M

EP2 uc3m

Introduction to ABEP

➢ Air-Breathing Electric Propulsion (ABEP)

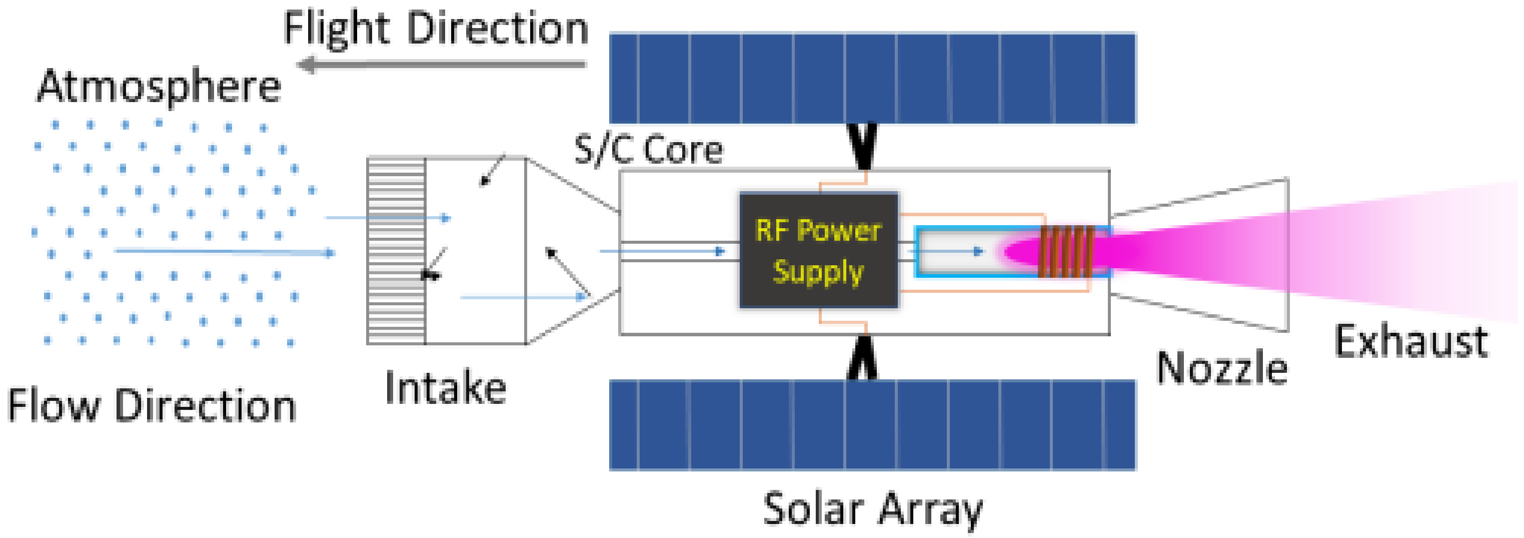

Romano, F. et al. (2017). Performance Evaluation of a Novel Inductive Atmosphere-Breathing EP System.

Advantages of HPT over HT

- No need for cathode or neutralizer.
- Typically operated at lower power.

Disadvantages of HPT over HT

- Less mature technology.
- Lower efficiencies, poor propellant utilization…

Introduction to ABEP

➢ Thesis objectives

Objectives

- Experimental analysis of alternative propellants in a **plasma thruster breadboard model**.
  - Characterization of the HPT operated with Air and Air-Kr mixtures.
- Experimental analysis of alternative propellants in a **plasma source breadboard model**.
  - Controlled RF discharges with air mixtures for ABEP validation, and ABEP-Kr assisted validation.
  - Design and improvement of plasma diagnostics for Air / Kr RF plasma.

Design modifications and ABEP-oriented optimization

Experimental setup

- HPT05M breadboard model jointly developed by SENER Aeroespacial and UC3M

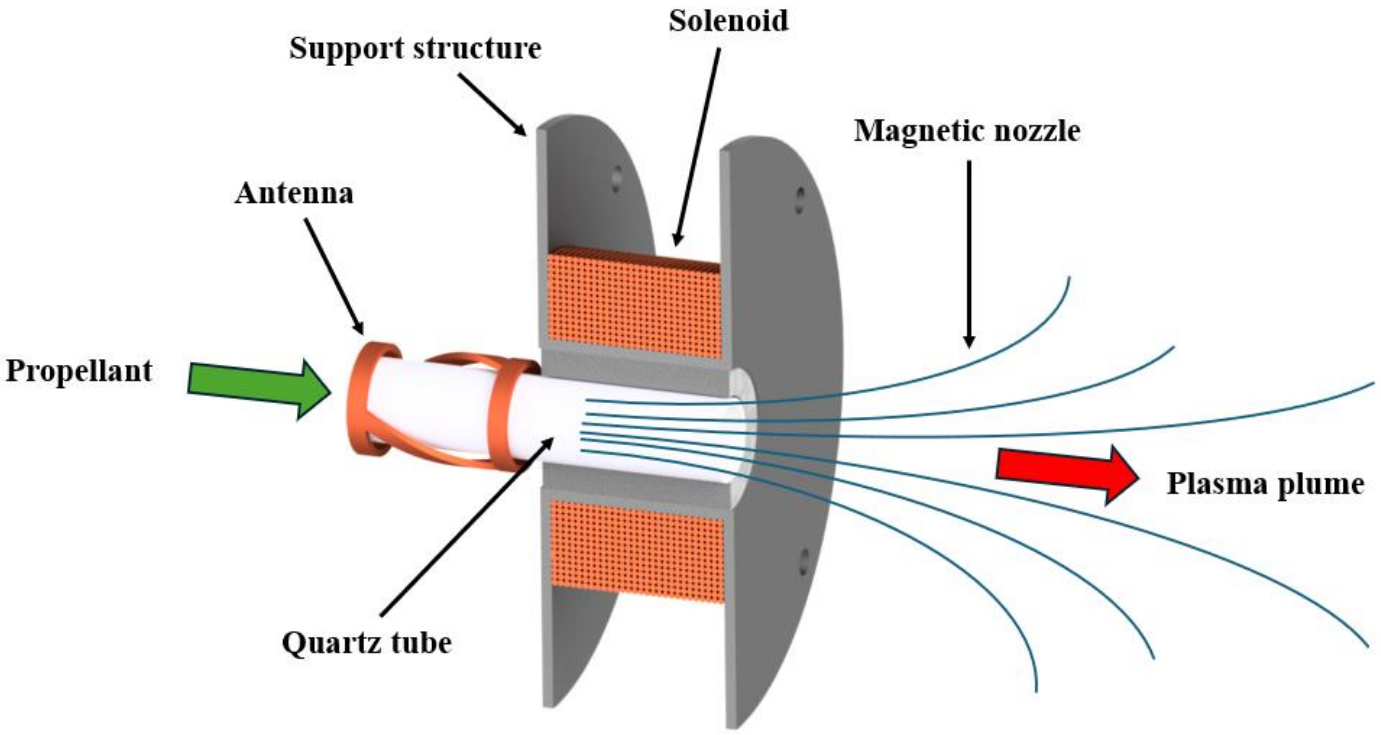

HPT05M	
Dimensions (diam, length)	25mm, 140mm
RF frequency	13.56 MHz
Power	300-450 W
Magnetic field	600-1200 G
Mass flow rate	4.5 – 22.5 sccm Air

Experimental setup

➢ Electrostatic probes

Faraday cup

- In-house developed.
- 10 mm aperture.
- Biased at -150 V.

Retarding potential analyzer

- Semion unit by Impedans.
- 4 grids (floating, -60V, 0-250V, -70V).
- Electrode collector at -60V

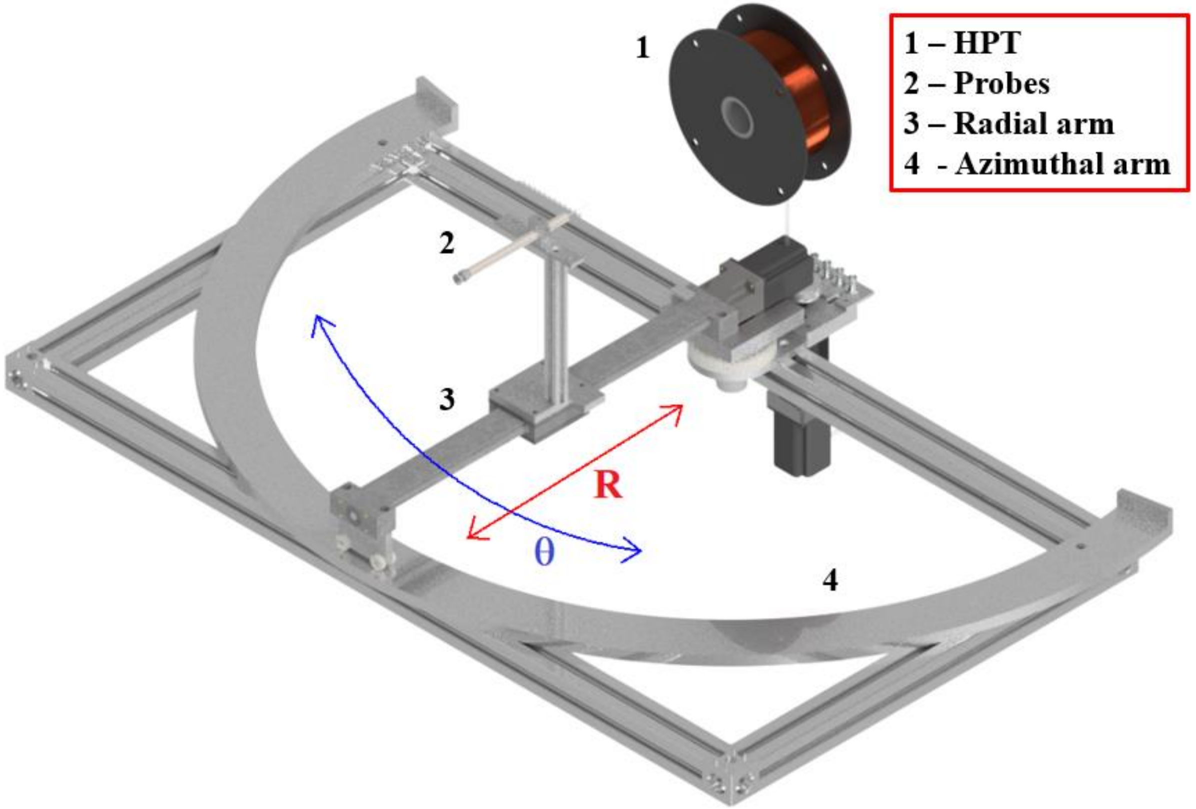

R ∈ (0, 400) mm
θ ∈ (-90, 90) deg

Experimental setup

- Thrust balance

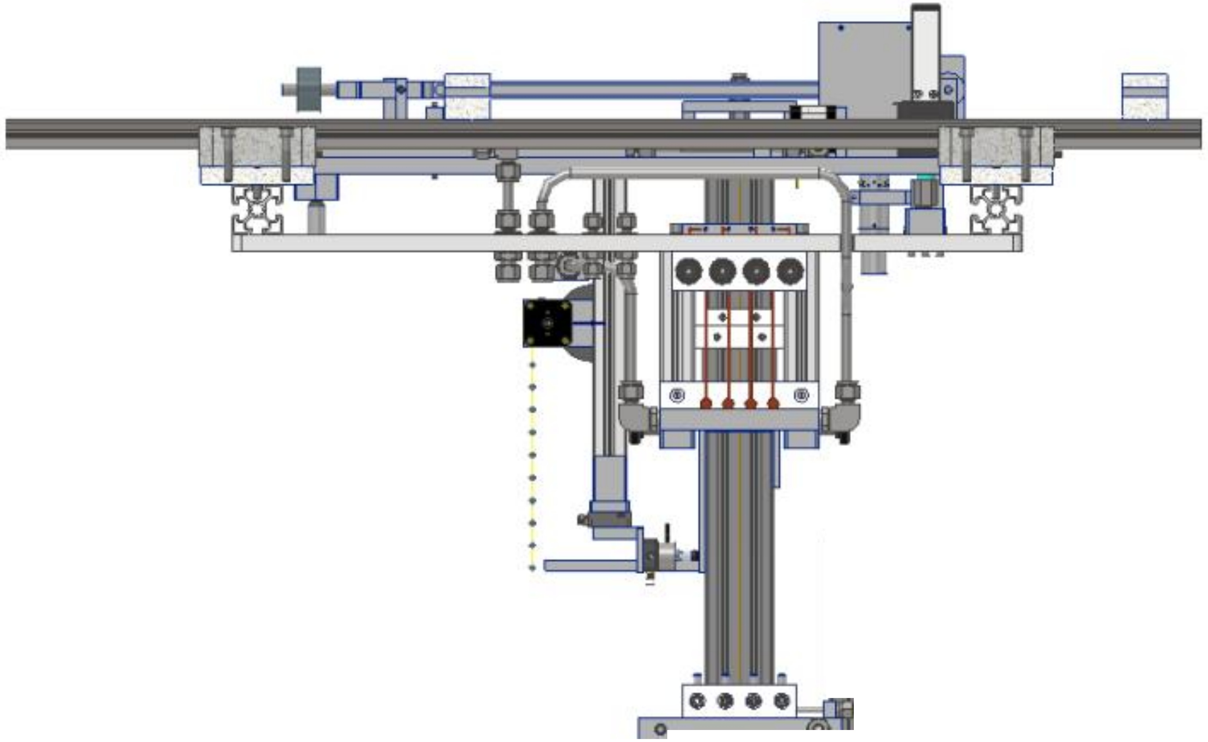

Inchingolo M. R, et al. (2022). Direct Thrust Measurements of a circular waveguide Electron Cyclotron Resonance Thruster

$$F_{TB} = \frac{L_{cal}}{L_t} k_{cal} y = \kappa_s y$$

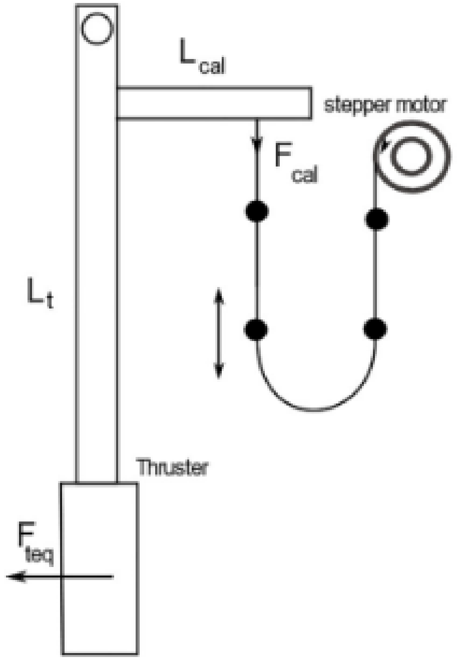

Plume composition impact

- Assumptions on the plume composition

$$\eta_u = \frac{I_b m_i}{\dot{m}} \qquad m_i = \sum_j \chi_j(\beta_{O_2}, \beta_{N_2}) m_j$$

Scenario	m_i (Da)
Full dissociation, $\beta_{O_2} = \beta_{N_2} = 1$	14.42
Null dissociation, $\beta_{O_2} = \beta_{N_2} = 0$	28.84
$\beta_{O_2} = 1, \beta_{N_2} = 0$	23.83
$\beta_{O_2} = 0, \beta_{N_2} = 1$	16.11
$\beta_{O_2} = \beta_{N_2} = 0.5$	19.22

Process	E_j (eV)
N_2 dissociation	9.76
N_2 ionization	15.58
N ionization	14.54
O_2 dissociation	5.16
O_2 ionization	12.07
O ionization	13.6

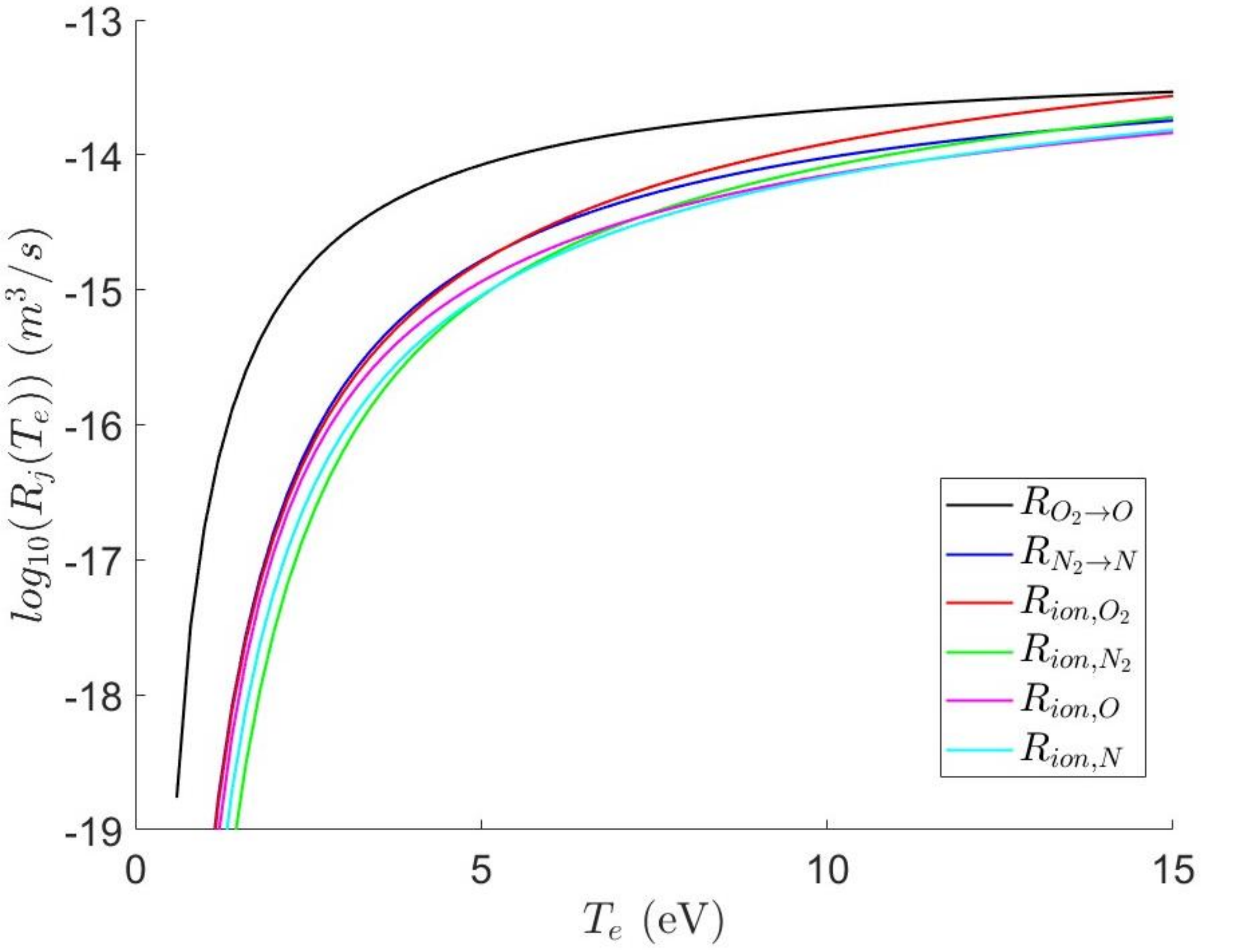

$$R_{O_2 \to O} > R_{N_2 \to N} > R_{ion,O_2} > R_{ion,O} > R_{ion,N} > R_{ion,N_2}$$

Results

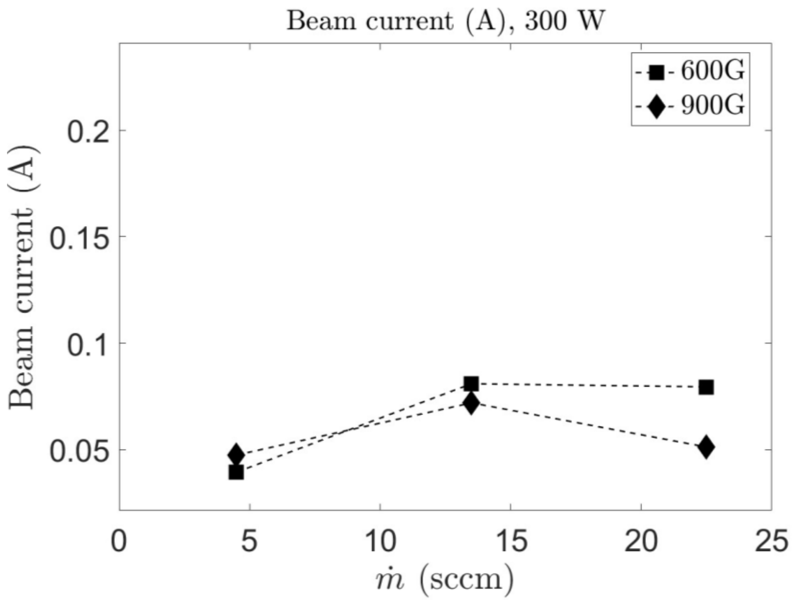

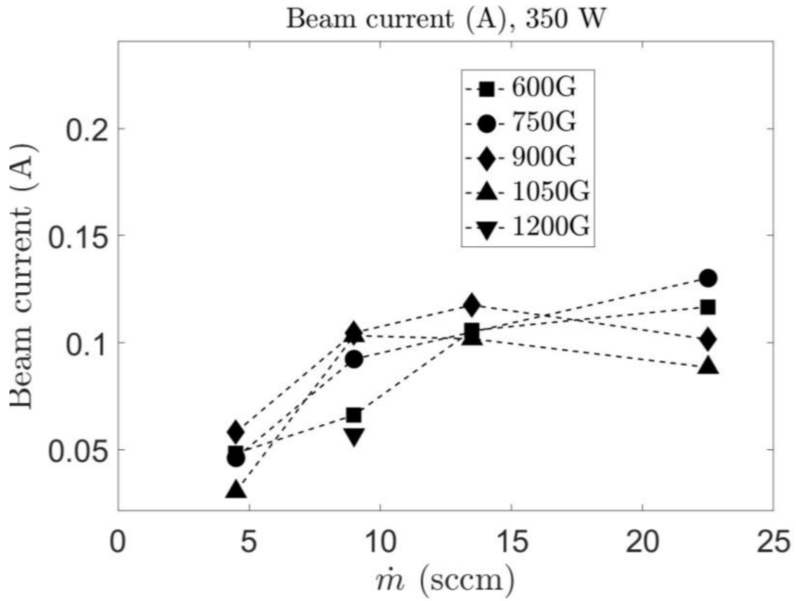

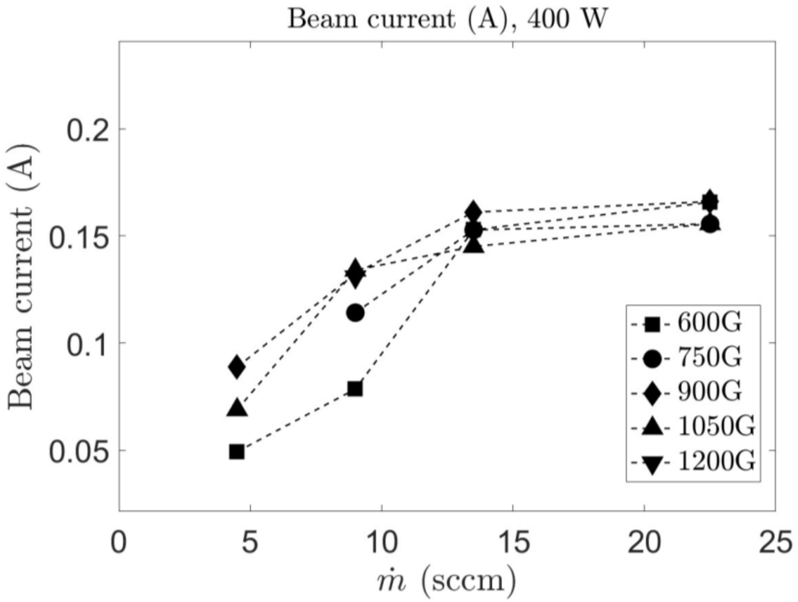

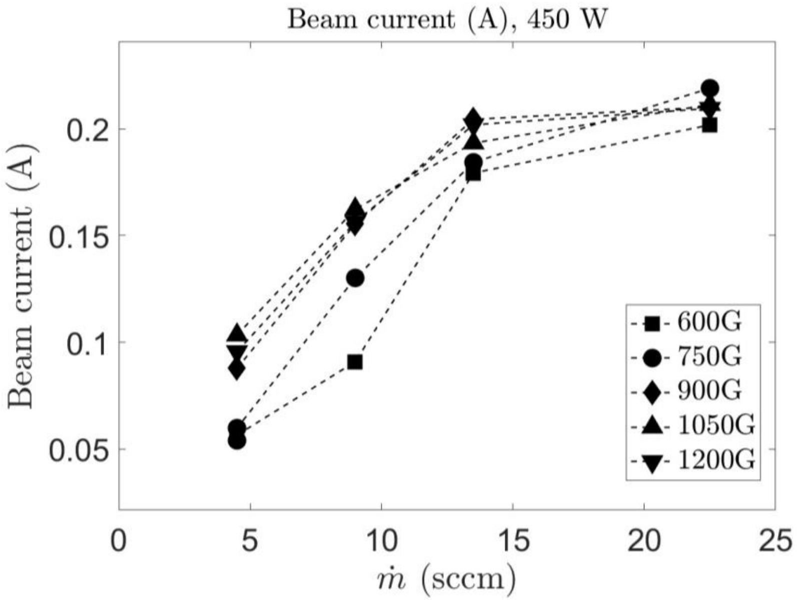

RF POWER EFFECT

- The current increases with the power.

MASS FLOW EFFECT

- Below ~13.5 sccmAir, the current increases.
- Above ~13.5 sccmAir, the current saturates.

MAGNETIC FIELD EFFECT

- The effect depends on the mass flow and the rf power.
- Can either increase or decrease the current, or not have any effect.
- In general, it is detrimental for low rf power and beneficial for high rf power.

Results

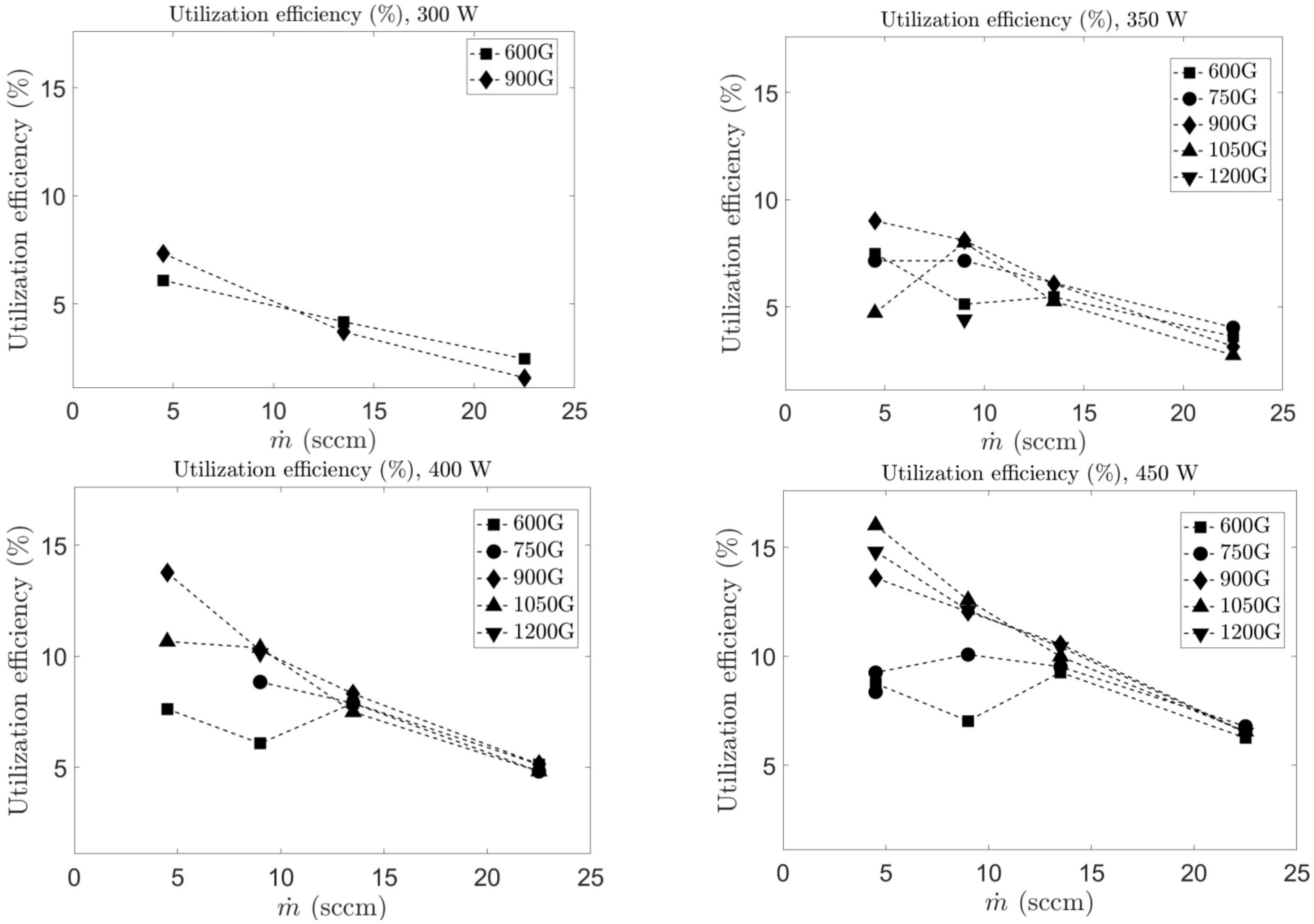

RF POWER EFFECT

- The utilization efficiency increases with the power.

MASS FLOW EFFECT

- The utilization efficiency, in general, decreases with the flow.

MAGNETIC FIELD EFFECT

- At high values of mass flow does not seem to have an effect.
- At low values, the contribution is not well understood.

Results

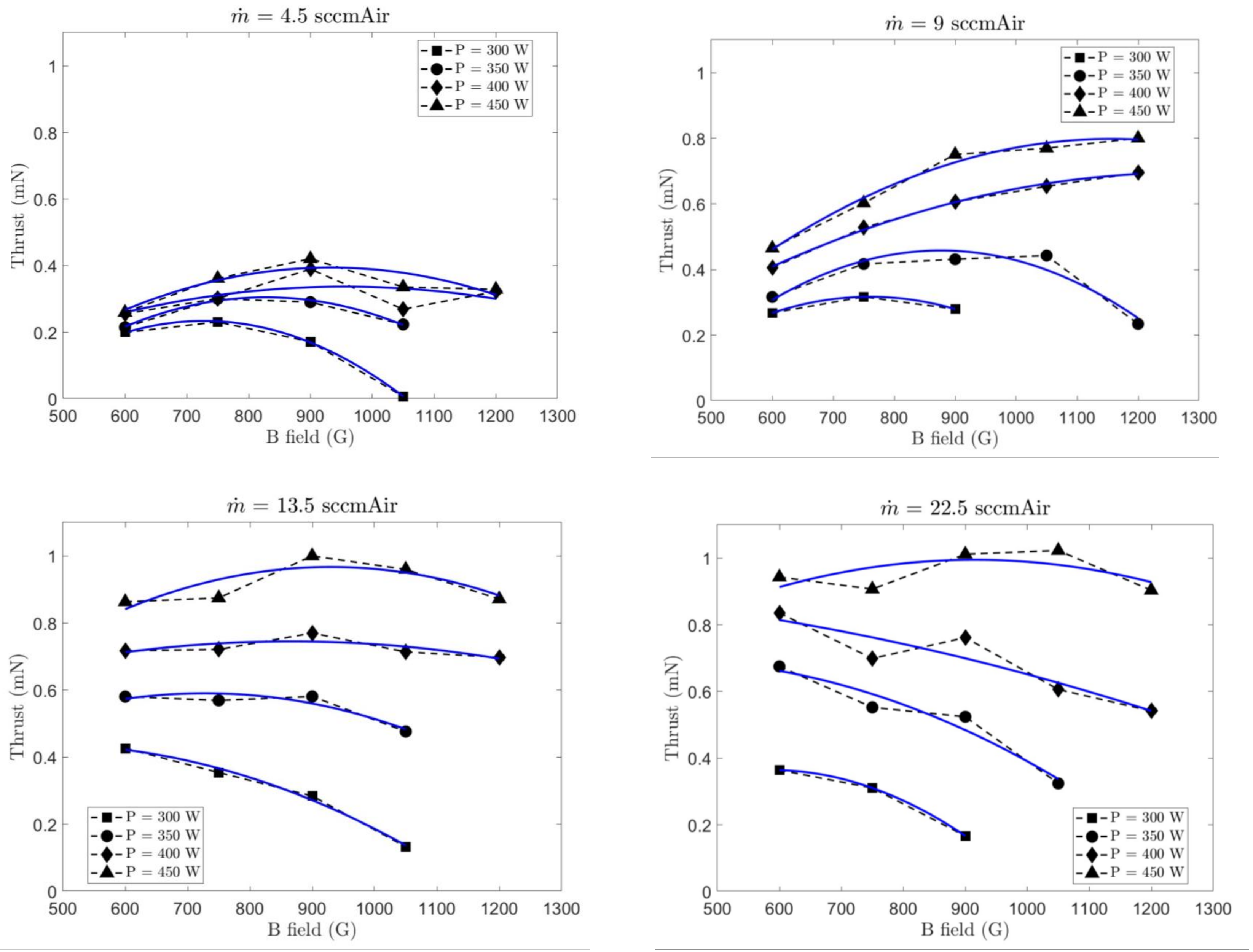

RF POWER EFFECT

- The thrust increases always, typically in a linear way.

MASS FLOW EFFECT

- Below ~13.5 sccmAir, the thrust increases.
- Above ~13.5 sccmAir, the thrust saturates.

MAGNETIC FIELD EFFECT

- The effect depends on the mass Flow and the rf power.
- Can either increase or decrease the thrust, or not have any effect.
- In general, it is detrimental for low rf power and beneficial for high rf power.

b-dot probe theory

- Objective
  - Measure the helicon wave in the plume.
  - Study the wave propagation and power coupling for different configurations.
- B-dot working priniciple
  - Faraday Induction Law: $\epsilon = -\frac{d\Phi_B}{dt}$
  - Ideally, $V_p = -NA\dot{B}_{tot}$
  - Sensitivity, $|\beta| = \left|\frac{V_p}{i\omega B_{ext}}\right| = \frac{NAZ_0}{|Z_{0+i\omega L}|}$

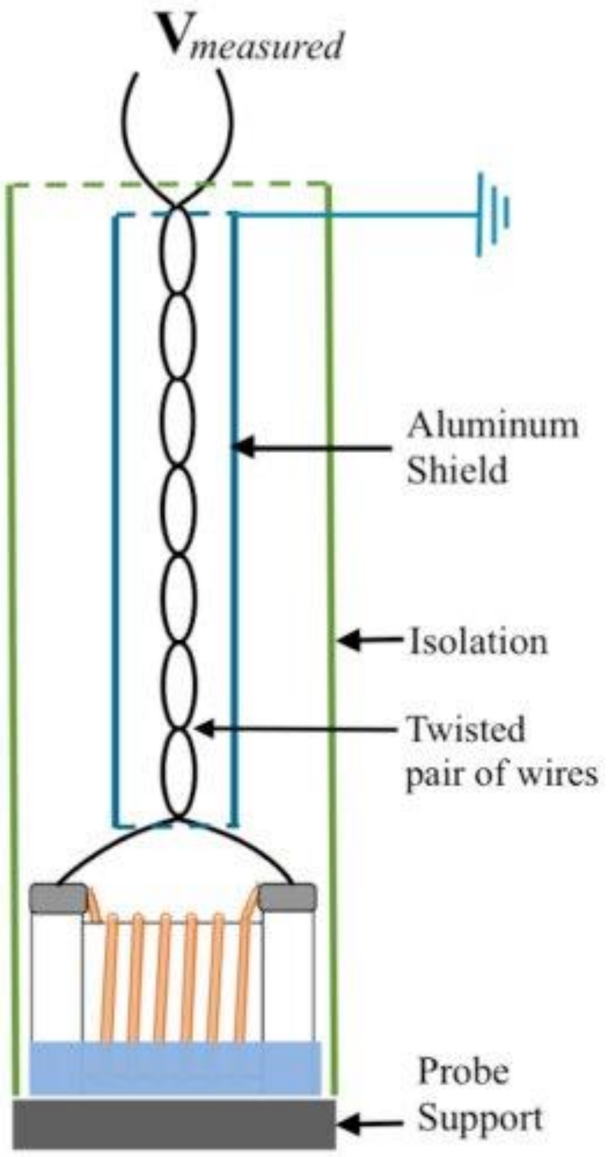

Manuel Azuara, et. al. (2019). Theoretical and Experimental Analysis for an Air-Breathing Pulsed Plasma Thruster

b-dot probe design

➢ Design & fabrication

- 3-axis b-dot probe: Designed so that every axis has the same sensitivity.
- r < 3 mm to ensure that the field is constant inside the loop.
- Aliminum foil as electric shield
- Electronics inside a Faraday Cage
- CTT for capacitive-pickup removal
- Dedicated L-type matching network
    - ~10% signal reflection at 13.56 MHz.

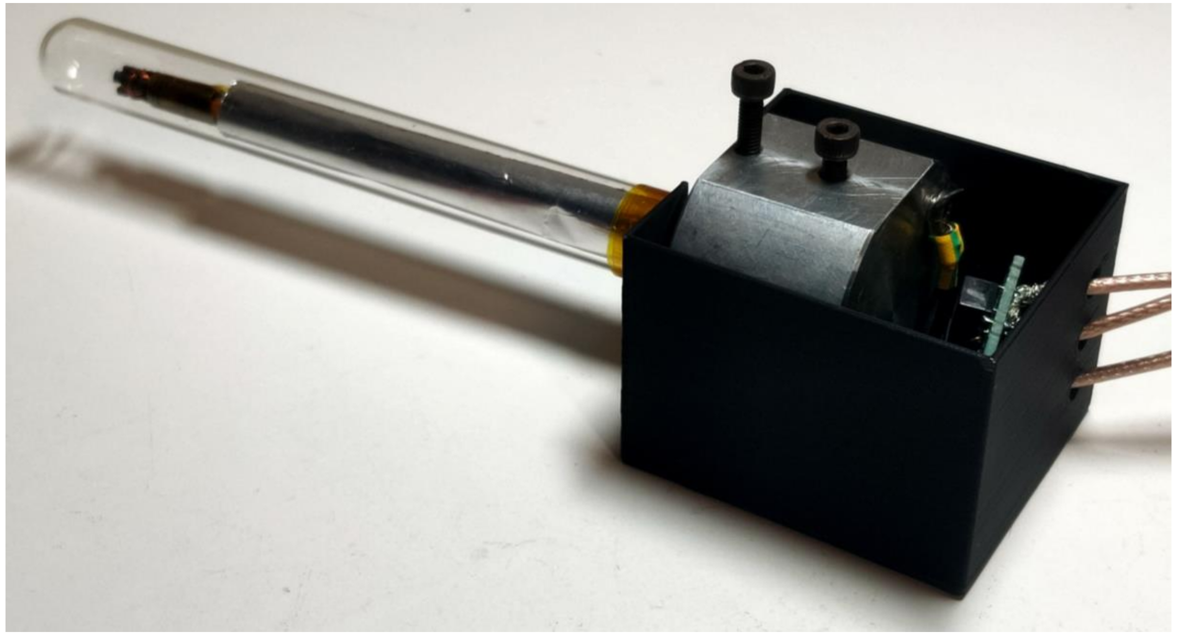

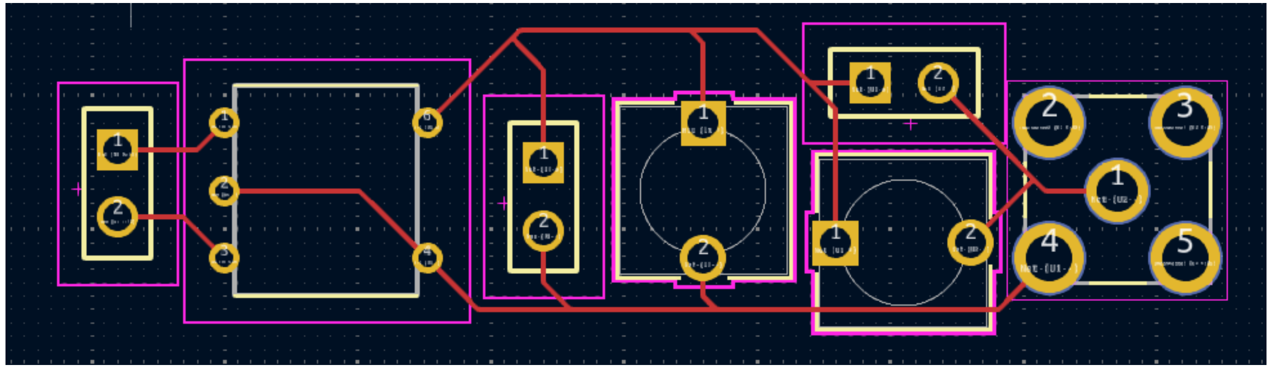

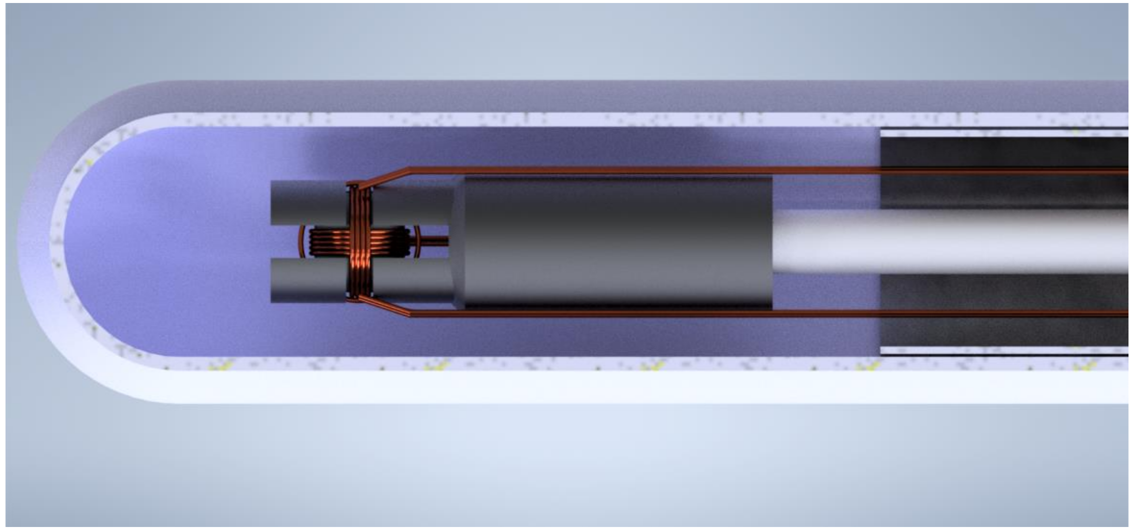

b-dot probe calibration

- Lots of lessons learnt. More complex than expected.
- Not trivial interaction with the calibration setup.

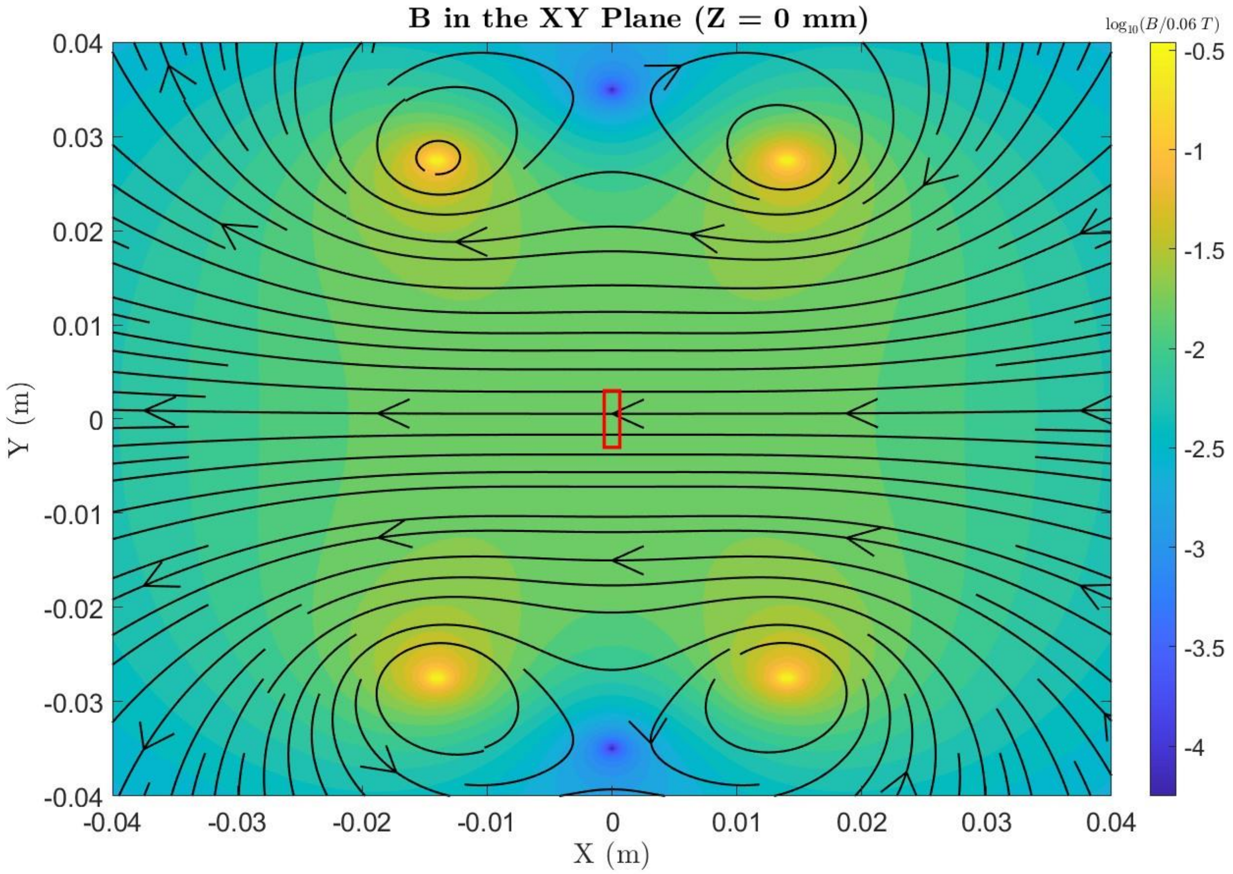

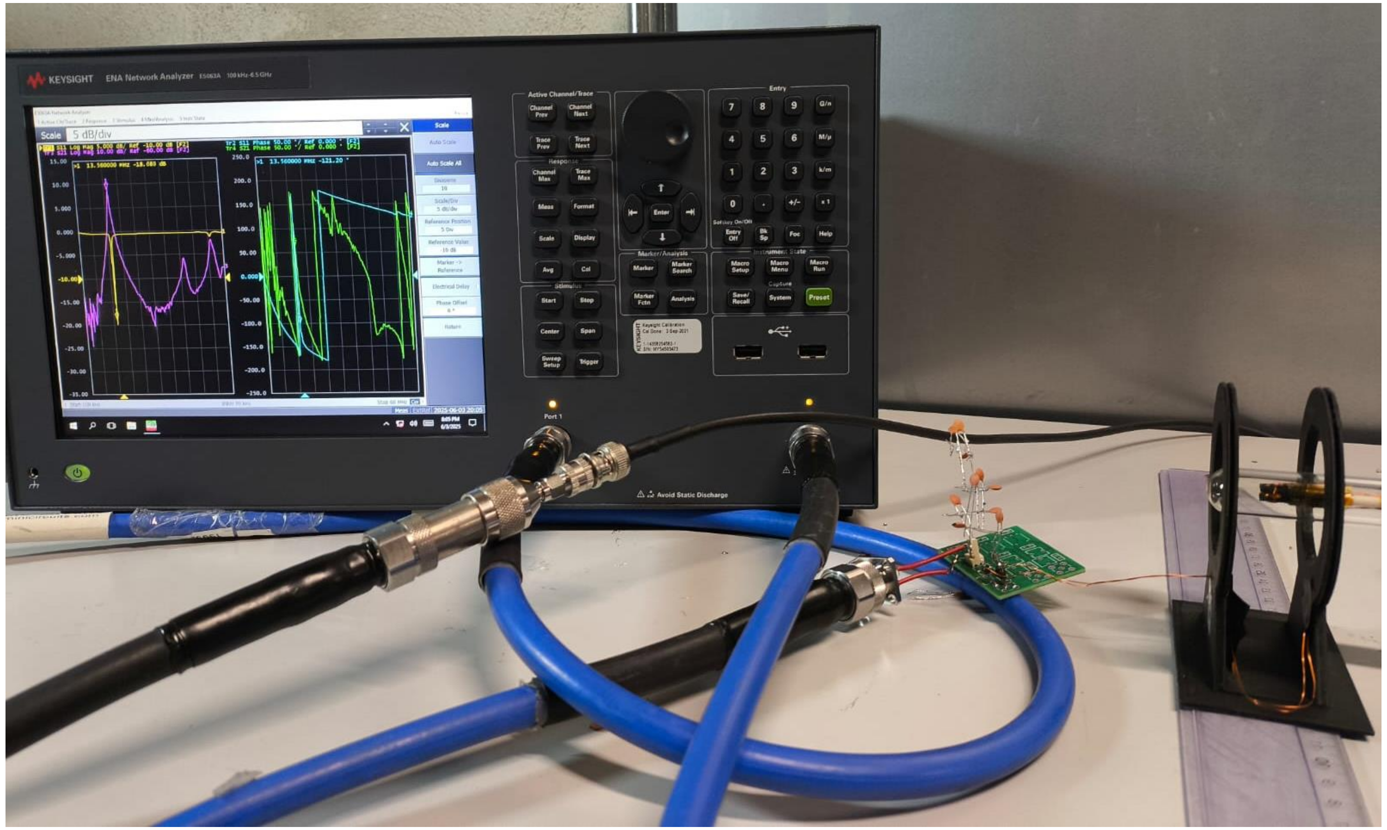

b-dot probe calibration

- $\beta = \frac{S_{21} Z_B}{2\pi i f \alpha (1+S_{11}) e^{i\varphi}}$

- Obtained sensitivity ~1 order of magnitud higher than the literature.

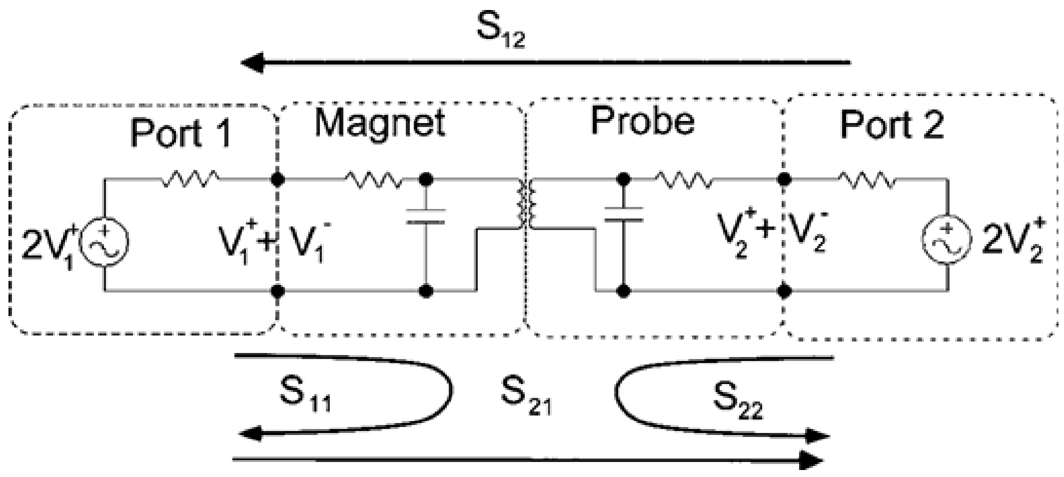

S. Messer, et. al. (2006). Broadband calibration of radio-frequency magnetic induction probes

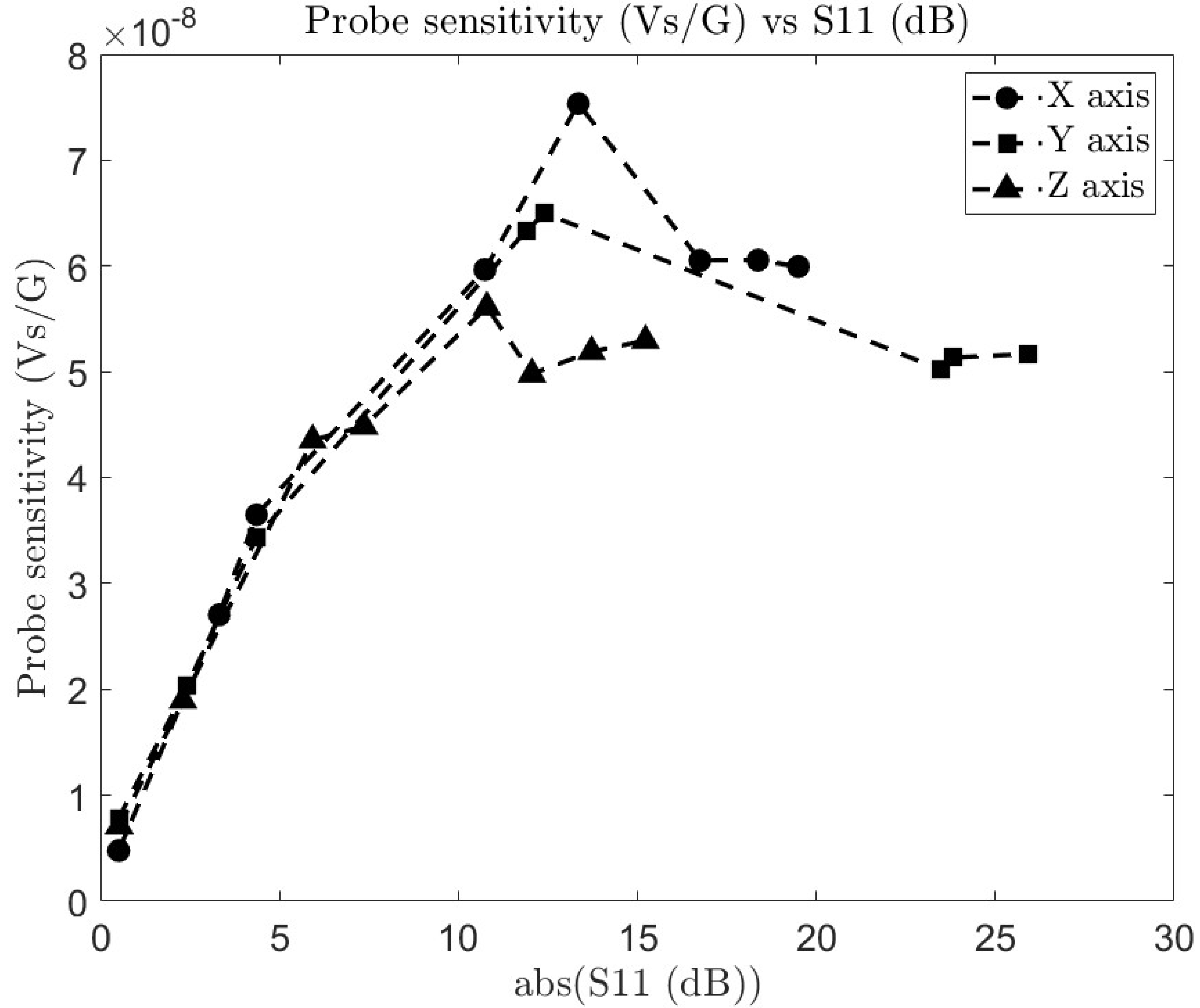

Conclusions & Future work

- First ABEP tests of our institution.
- First direct thrust measurements in an HPT operating with air.
- It might be necessary to have the ability to modify in orbit both the rf power and the magnetic field intensity.
- The calibration of a b-dot probe requires careful control of all the setup.

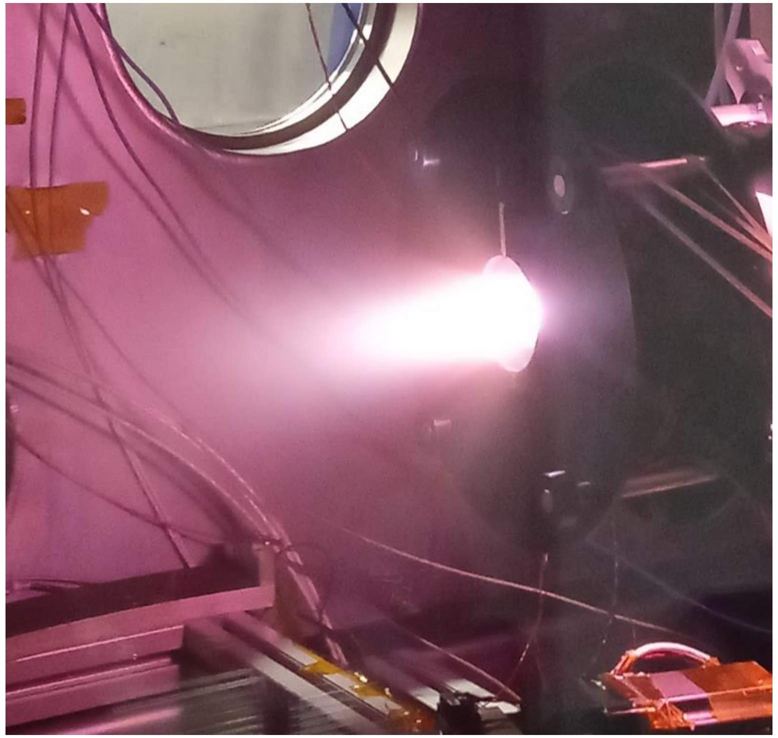

- Perform b-dot measurements for different conditions.
- 0-D global model for the composition of the plume.
- Use optical emission spectroscopy and the corresponding C-R model.
- Drag vs Altitude model.
- Optimize the thruster design to be used with Air.

Thank you! Questions?

email: ep2@uc3m.es
web: ep2.uc3m.es

EP2 uc3m

BACKUP SLIDES

Results

P = 400 W, B = 600 G

➢ Ion current density

- The center peak increases up to ~13.5 sccm Air.
- Increasing ṁ leads to an increase in the side lobes.
- More j_i than in the Krypton case for the same particle flow rate.

Confirms that the dissociation events probably dominate the plasma

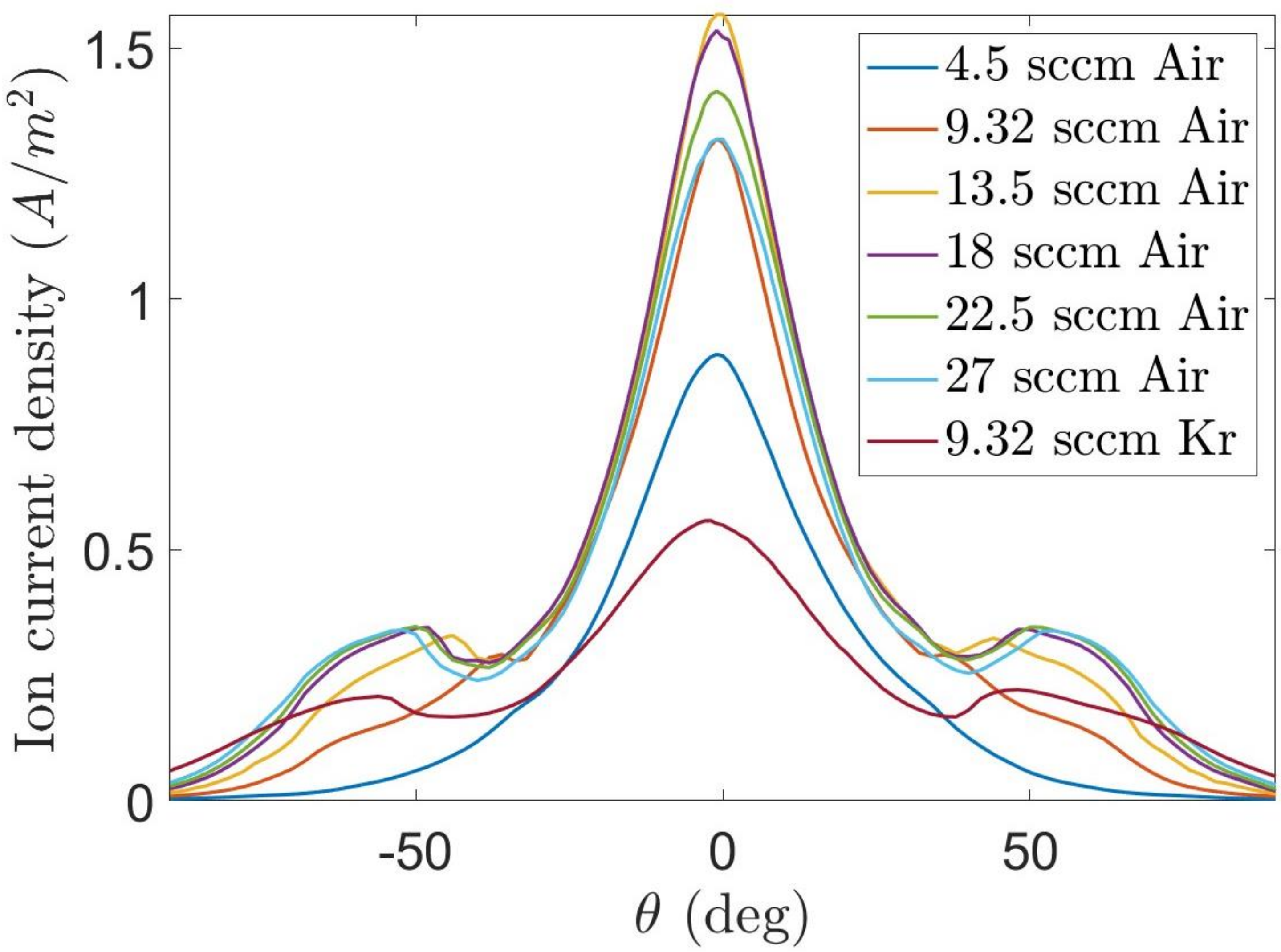

Results

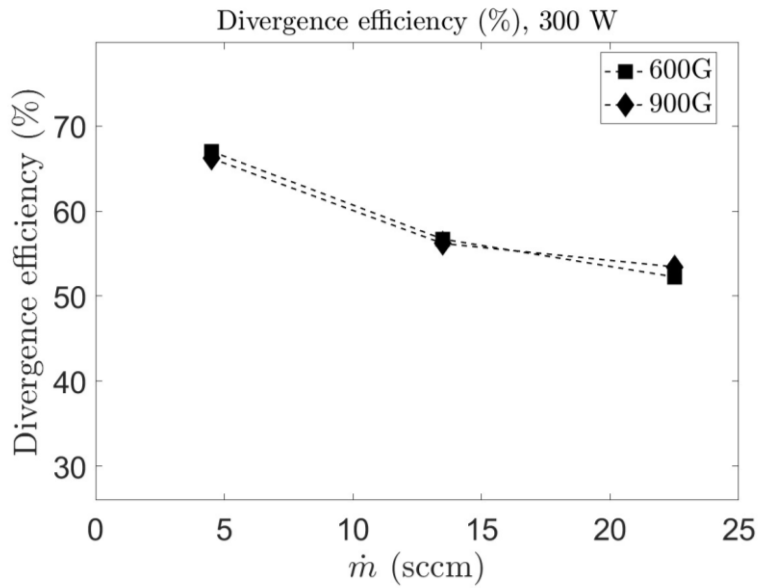

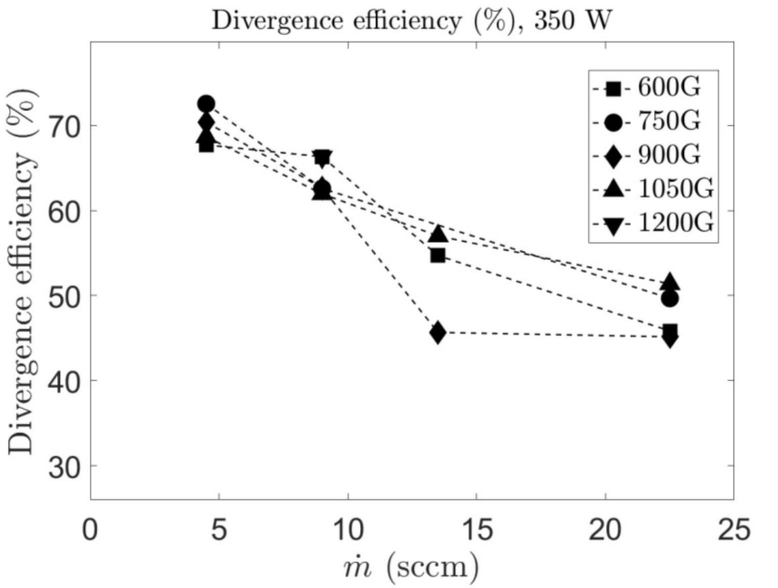

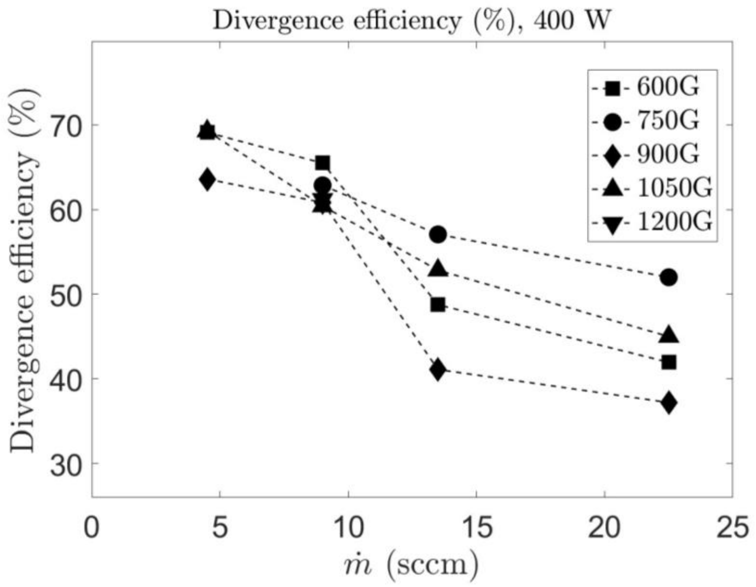

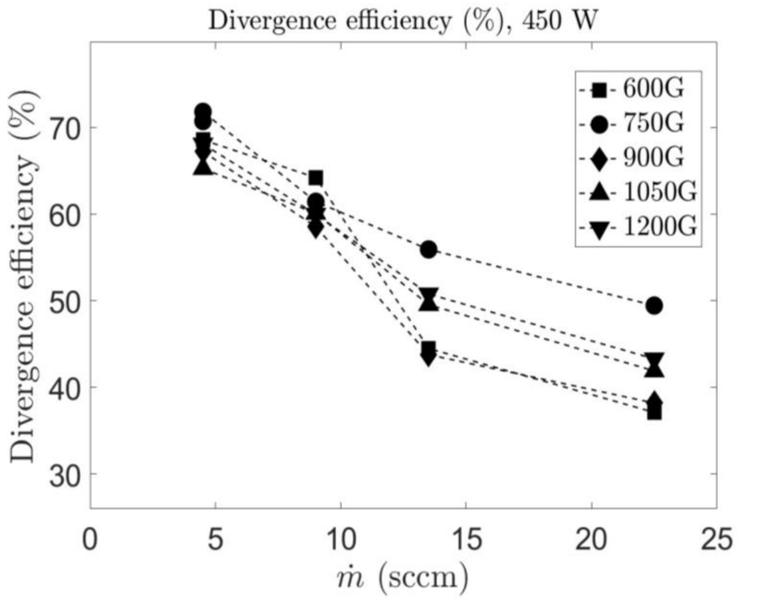

RF POWER EFFECT

- Does not seem to have any remarkable impact, but it provoques a slight decrease.

MASS FLOW EFFECT

- Decreases with flow.

MAGNETIC FIELD EFFECT

- At low flows has little impact.
- At high flows, high powers has a great impact, although the relation is not trivial.

Results

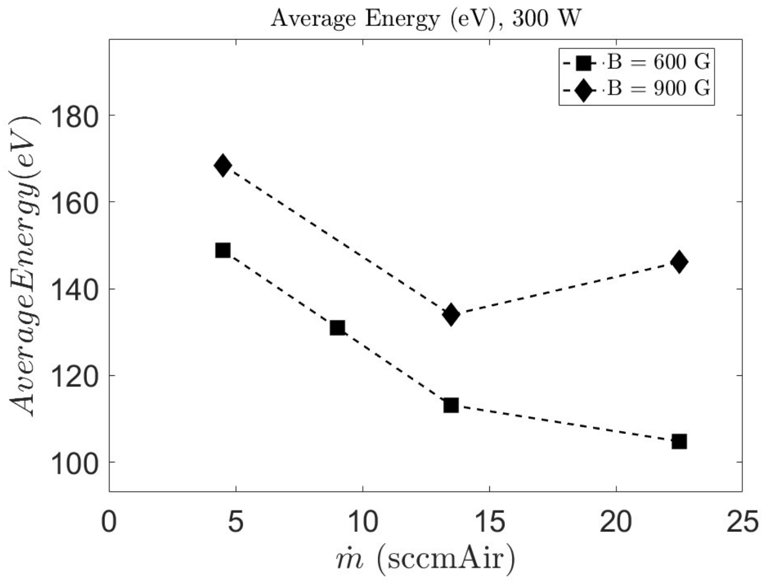

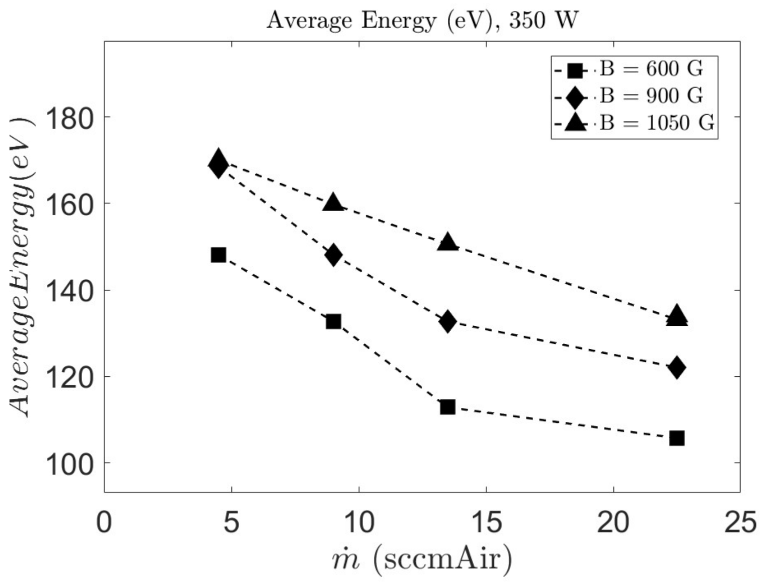

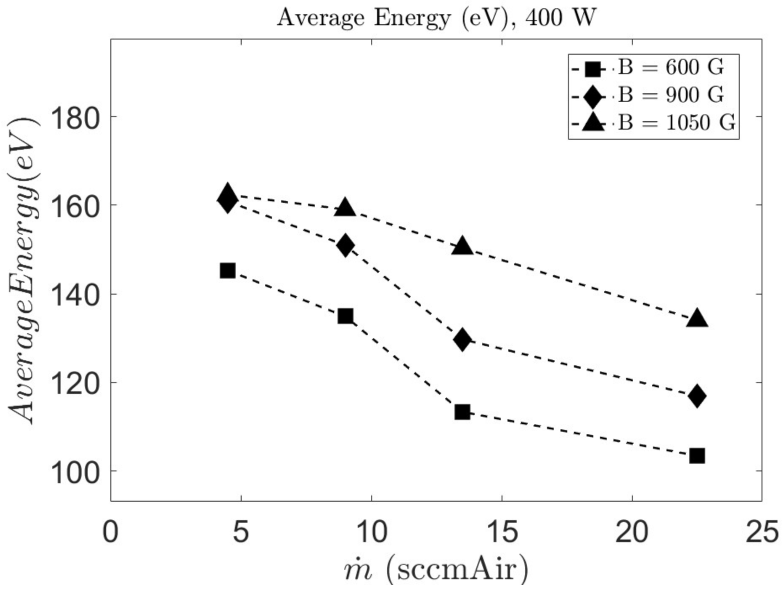

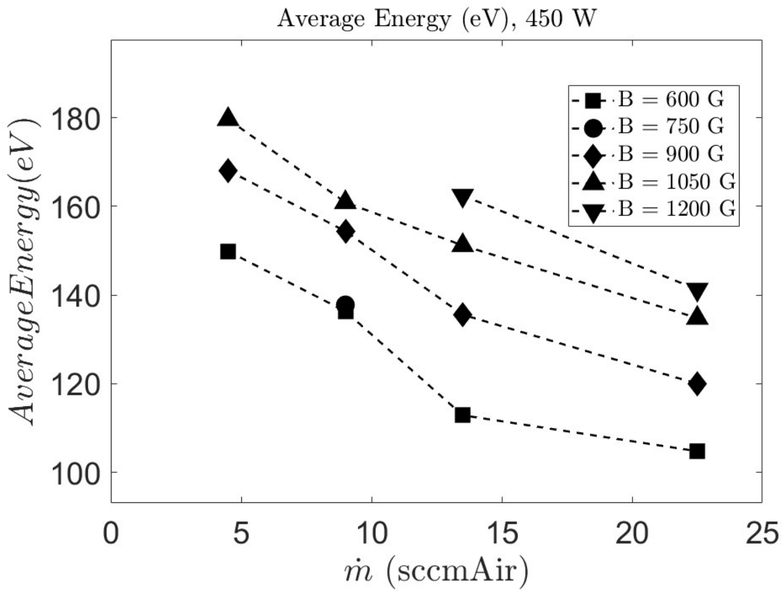

RF POWER EFFECT

- Does not seem to have any remarkable impact.

MASS FLOW EFFECT

- Decreases with flow.

MAGNETIC FIELD EFFECT

- Increases the energy in all cases.

Initial feasibility study

➢ Drag vs Altitude Model

- $A_{int} = \frac{\dot{m}}{\eta_{int}\rho v}$
- $L_{sat} = \frac{A_{int}}{4\pi f_{length}} + L_{thruster}$
- $A_l = 2A_{panels} = \frac{P_{sat}+P_{rf}+P_{solenoid}}{\eta_{panel}E_{sun}}$
- $R_{sat} = \frac{A_l}{2\pi L_{sat}}$
- $A_{front} = \pi R_{sat}^2$
- $D = \frac{1}{2}\rho v^2 \left\{C_{D_{par}} A_l + C_{D_{perp}}\left[A_{front} - (1-\beta)A_{int}\right]\right\}$

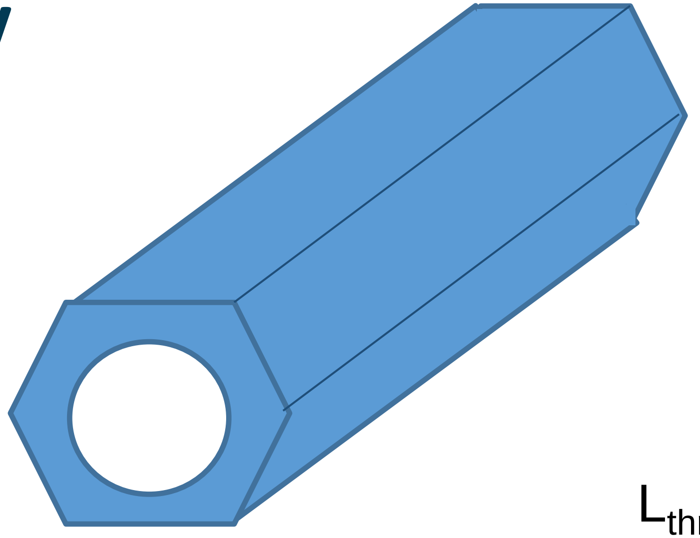

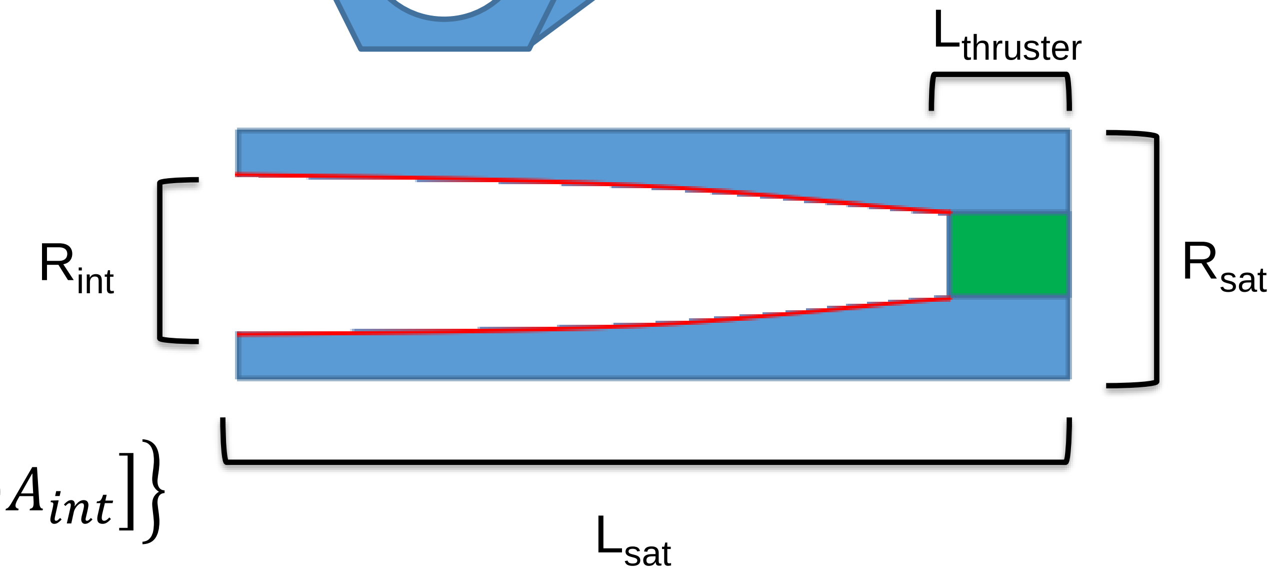

Initial feasibility study

- Input parameters
  - $\eta_{int} \in [0.5, 1]$
  - $\beta_{int} \in [0, 1]$
  - Solenoid or Permanent Magnet
  - P_{sat} = 1 kW
  - $\eta_{panel} = 0.3$
  - Max dimensions -> Miura 5 fairing
    - r_{max} = 0.825 m
    - L_{max} = 2.97 m

Scenario	Power (W)	Mass flow (sccmAir)	Field (G)	Altiude (km)	Free volume (m^3)
SOL_1_0	400	13.5	600	297.5	1.0245
PM_1_0	450	13.5	900	292.5	0.8334

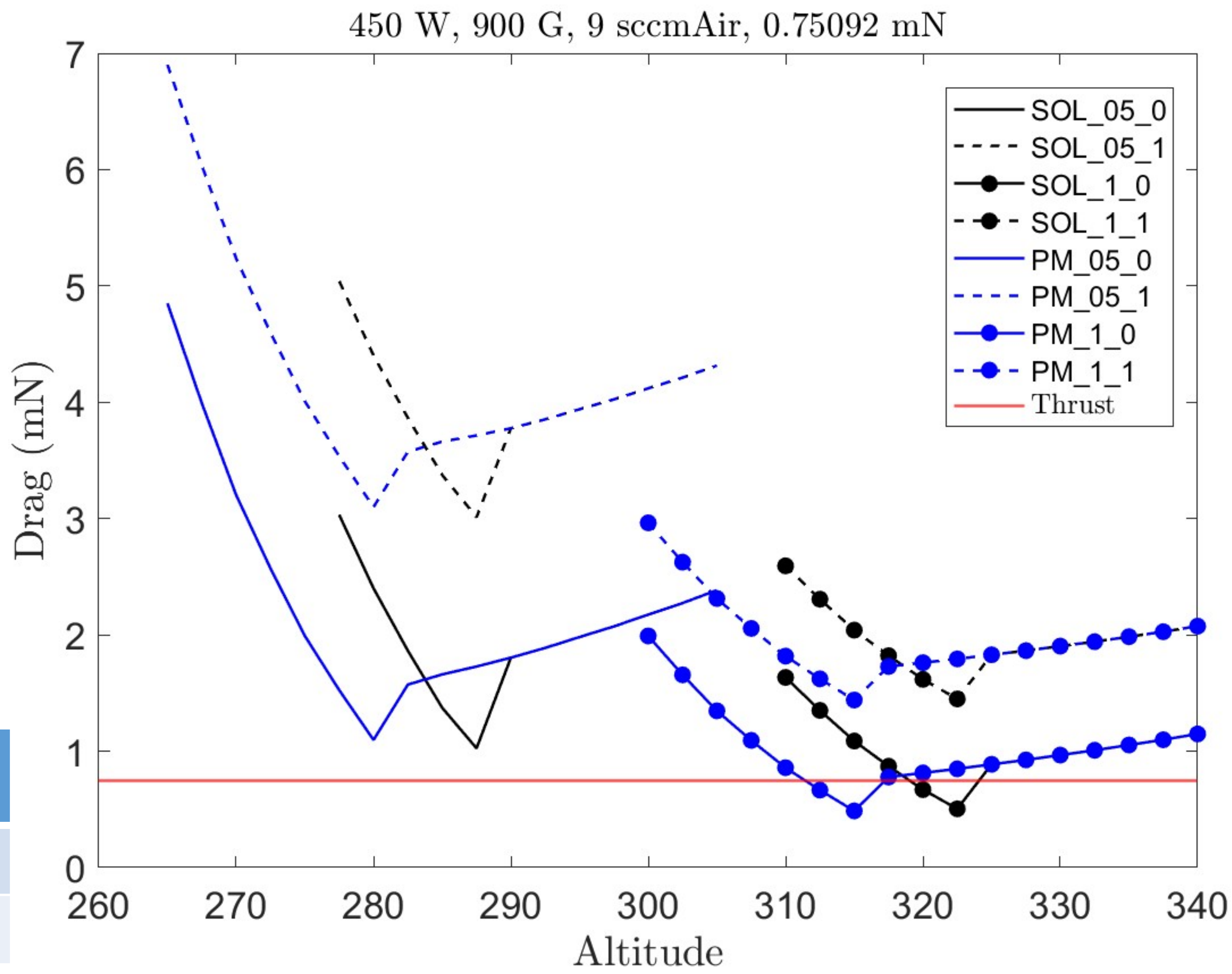

Experiments & Results

➢ Thrust calibration methodology

We have to correct the measurement to remove the termal drift and other low-frequency oscillations

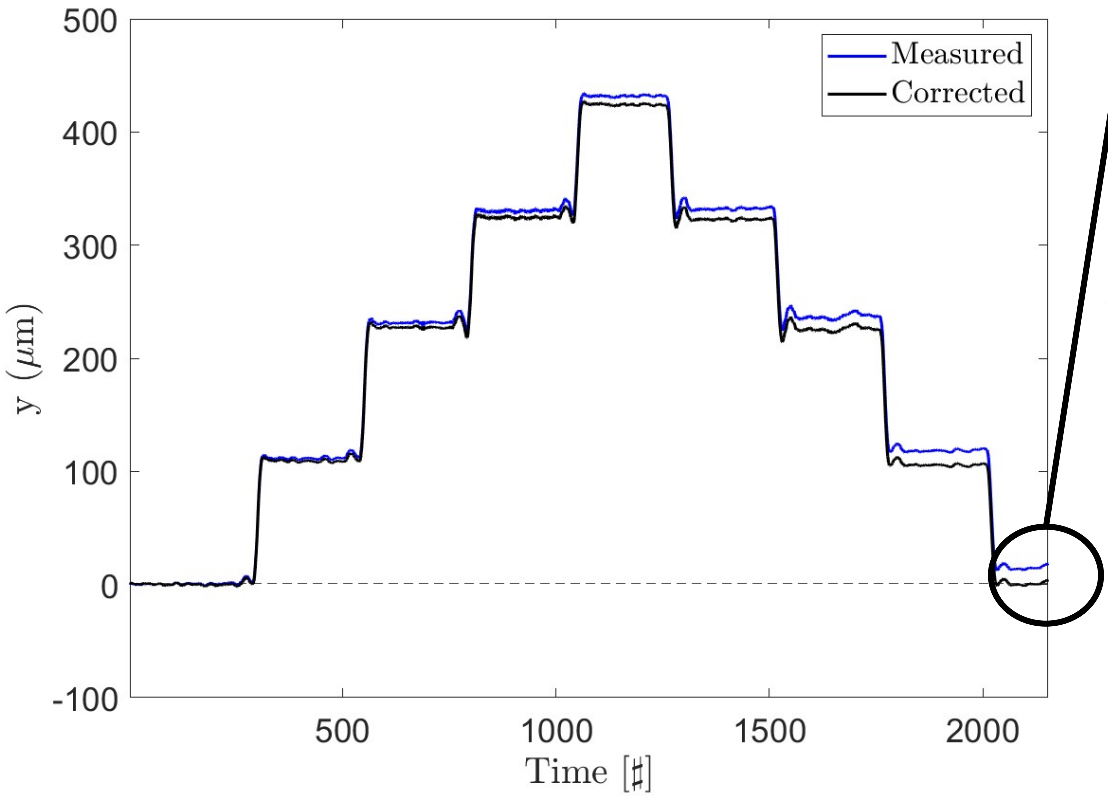

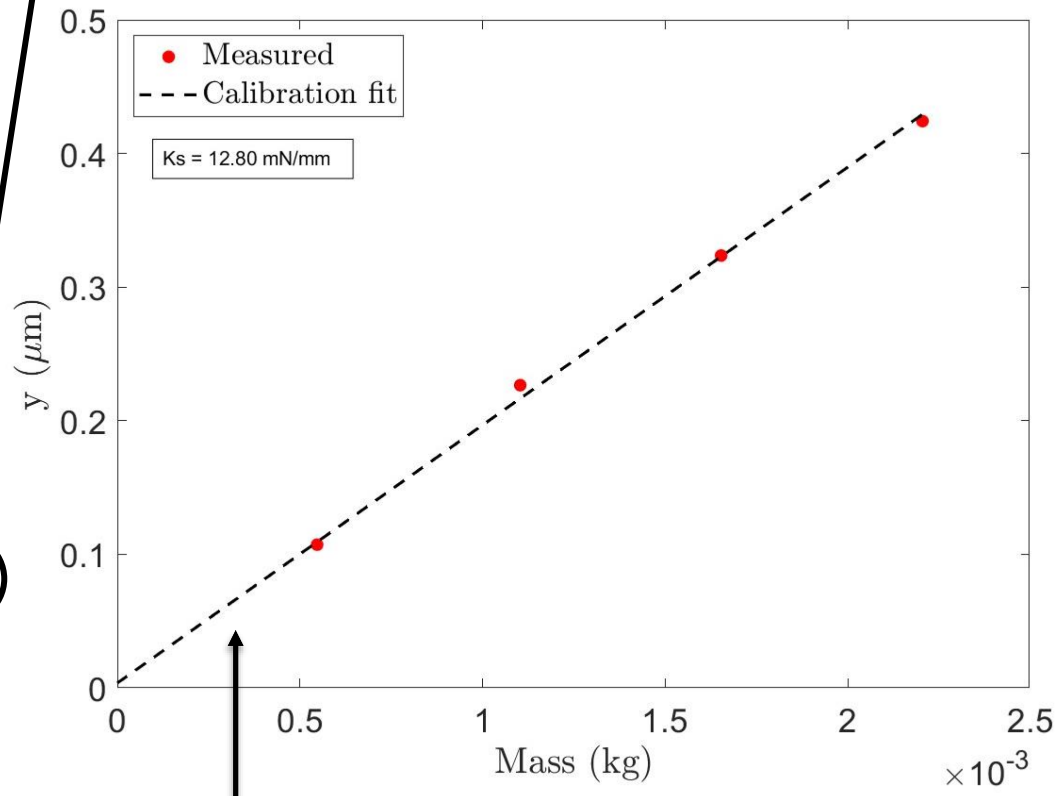

K_s is the slope of the mass-displacement plot

Experiments & Results

➢ Thrust measurement methodology